Cardiovascular Innovations and Applications

Vol. 9 (2024) 21
ISSN 2009-8618
DOI 10.15212/CVIA.2024.0012

RESEARCH ARTICLE

Prognostic Value of Optical Flow Ratio among Patients with Coronary Artery Disease after Percutaneous Coronary Treatment: A Hospital-Based Retrospective Cohort Investigation

Chuliang Hong[1,2,a], Sicheng Chen[3,a], Tianyu Hu[4], Zehuo Lin[1], Pengyuan Chen[1], Zijing Lin[1], Lixin Xie[5], Yuanhui Liu[1] and Pengcheng He[1,6]

[1]*Department of Cardiology, Guangdong Provincial People's Hospital (Guangdong Academy of Medical Sciences), Southern Medical University, Guangzhou 510080, China*
[2]*Department of Cardiology, The Tenth Affiliated Hospital of Southern Medical University (Dongguan People's Hospital), Dongguan, China*
[3]*Department of Cardiology, Shantou Central Hospital, Shantou, China*
[4]*Department of Catheterization Lab, Guangdong Cardiovascular Institute, Guangdong Provincial Key Laboratory of South China Structural Heart Disease, Guangdong Provincial People's Hospital (Guangdong Academy of Medical Sciences), Southern Medical University, Guangzhou 510080, China*
[5]*Department of Cardiology, Shangyou People's Hospital, Ganzhou, China*
[6]*Department of Cardiology, Heyuan People's Hospital, Heyuan, China*

Received: 1 October 2023; Revised: 15 December 2023; Accepted: 16 January 2024

Abstract

Objective: The goal of this study was to examine the prognostic performance of optical flow ratio (OFR) among patients with coronary artery disease (CAD) after percutaneous coronary intervention (PCI).
Methods: We recruited patients with CAD undergoing optical coherence tomography (OCT)-directed PCI between January 2019 and June 2021 for our single-center, hospital-based, retrospective cohort investigation. We assessed the link between post-PCI OFR and major adverse cardiovascular events (MACE) via multivariate Cox regression analysis.
Results: Receiver operating characteristic analysis revealed that the best post-PCI OFR threshold for MACE was 0.91, and introduction of OFR into the baseline profile and OCT results markedly enhanced MACE identification after PCI. On the basis of survival curves, patients with OFR ≤0.91 ($P < 0.001$) and thin-cap fibroatheroma (TCFA) ($P = 0.007$) exhibited higher MACE incidence, and myocardial infarction (MI) incidence was considerably greater among patients with OFR ≤0.91 ($P < 0.001$), compared with OFR >0.91. Multivariate Cox regression analysis suggested that OFR ≤0.91 (hazard ratio [HR]: 3.60; 95% confidence interval [CI]: 1.24–10.44; $P = 0.019$), and TCFA (HR: 3.63; 95% CI: 1.42–9.20; $P = 0.007$) were independent risk factors for MACE, and OFR ≤0.91 was independently associated with MI (HR: 14.64; 95% CI: 3.27–65.54; $P < 0.001$).
Conclusion: OFR after PCI is an independent MACE bio-indicator among patients with CAD. Adding OFR to post-PCI OCT results may potentially enhance MACE prediction.

Keywords: optical flow ratio; coronary artery disease; percutaneous coronary intervention; major adverse cardiovascular events

Introduction

Percutaneous coronary intervention (PCI) is a critical and necessary intervention for patients with coronary artery disease (CAD) [1]. Intracoronary optical coherence tomography (OCT), with markedly enhanced resolution, provides more detailed coronary artery morphology visualization than conventional two-dimensional coronary angiography and therefore is increasingly used in PCI [2]. Prior investigations have revealed that fractional flow reserve (FFR)-based strategies of coronary lesion functional estimation have superior performance, with the potential to enhance patient outcomes [3–5]. The optical flow ratio (OFR), an OCT-based technique of physiological coronary stenosis assessment, exhibits augmented diagnostic accuracy both before and after PCI [6]. More recently, post-PCI OFR has been reported to be an independent indicator of target vessel failure among patients with acute coronary syndrome (ACS) [7]. However, only limited studies have examined the clinical relevance of OFR after PCI among patients with CAD. Hence, we examined the influence of OFR after PCI on the cardiovascular prognosis of patients with CAD.

Methods

Study Design and Population

This single-center, hospital-based, retrospective cohort investigation explored the correlation between post-PCI OFR and cardiovascular prognoses among patients with CAD. We recruited patients from Guangdong Provincial People's Hospital between January 2019 and June 2021. This study included patients with (1) confirmed CAD diagnosis, as evidenced by coronary angiography, who also received OCT-directed PCI, and (2) clear and analyzable post-PCI OCT images. Patients with (1) no coronary artery stent implantation, (2) no available post-PCI OCT images, (3) missing analyzable post-PCI OCT images, owing to inferior image quality, and (4) less than 1 year of follow-up were excluded. Our work received ethical approval from Guangdong Provincial People's Hospital, and the need for informed consent from the study participants was waived.

OCT Image Analyses and Descriptions

We obtained OCT images after PCI by using a frequency-domain OCT system (ILUMIEN™ OPTIS™; Abbott Vascular, Santa Clara, CA, USA) and Dragonfly™ OPTIS™ imaging catheters. Catheters were placed approximately 5–10 mm distal to the target stents and were removed immediately after luminal blood evacuation with contrast media for OCT image capture purposes. The acquired images were digitally saved for offline analyses by two highly skilled researchers blinded to the patients' clinical and coronary angiographic information.

The target vessel (TV) was categorized into longitudinal subsegments as follows [7]: (1) stented, (2) adjoining reference (≤5 mm long), and (3) nonculprit lesion (Figure 1).

Stent expansion was described as the stent area divided by the average luminal reference area [8]. In-stent irregular protrusion referred to an irregularly structured material protruding into the lumen between stent struts [9, 10]. Moreover, because struts are occasionally found within the intima, only protrusions with a maximum height ≥200 μm were included in our analysis [9]. Stent malapposition was described as a marked delineation (≥200 μm) between struts and vessel wall [2, 11]. Stent edge dissection (SED) referred to an evident stent edge flap-mediated interruption in the luminal surface [9]. Finally, thin-cap fibroatheroma (TCFA) referred to a plaque composed of ≥180° lipid arc and ≤65 μm fibrous cap thickness [10, 12].

OFR Computation and Plaque Characterization Analysis

We used OctPlus software 1.0 (Pulse Medical Imaging Technology, Shanghai, China) for OFR computation and automated plaque characterization,

[a]Chuliang Hong and Sicheng Chen contributed equally to this work.

Correspondence: Yuanhui Liu and Pengcheng He, Department of Cardiology, Guangdong Provincial People's Hospital (Guangdong Academy of Medical Sciences), Southern Medical University, Guangzhou 510080, China, Tel: +86-20-83819161; Fax: +86-20-83824369, E-mail: lyh0718@126.com; gdhpc100@126.com

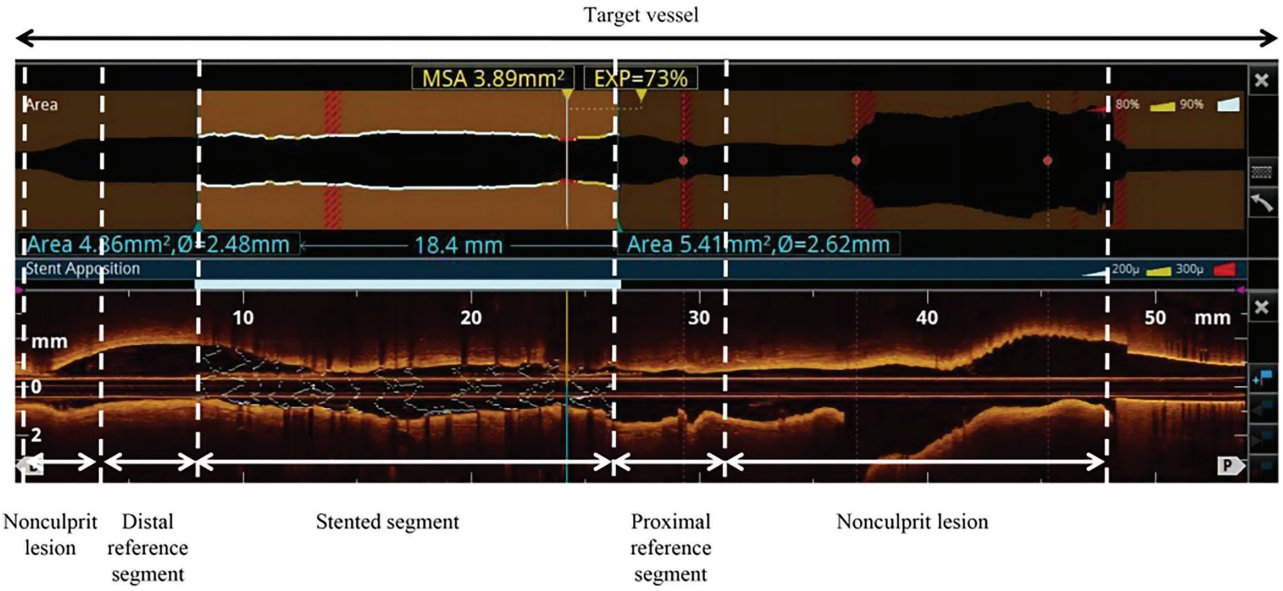

Figure 1 TV Subsegments Analyzed with OCT.
EXP: stent expansion; MSA: minimum stent area; OCT: optical coherence tomography; TV: target vessel; ø: lumen diameter of the reference segment of the target vessel.

as reported previously [13–15]. The software automatically contoured the coronary artery lumens in all OCT cross-sectional images. Subsequently, the section perpendicular to the automatically detected side branch center line was reconstructed, and the side branch ostium area was computed [13]. The reference luminal area was determined from the bifurcation fractal law [14] as well as the area conservation model, and the OCT proximal reference luminal area was multiplied by a virtual hyperemic flow rate of 0.35 m/s to achieve the virtual volumetric flow rate at the entrance boundary. Ultimately, the OFR values were computed along the reconstructed vessels with a novel technique adapted from the established formula for computing FFR. In addition, the reconstructed arteries were color-coded with the computed OFR values [15]. Plaque composition, i.e., the lipidic, fibrous, and calcific tissues, were then detected and quantified in the software. The aforementioned results were computed by a skilled researching blinded to the patient clinical outcomes [12, 16].

Outcomes

The main endpoint was major adverse cardiovascular events (MACE), integrating all-cause mortality (ACM), myocardial infarction (MI), and TV revascularization (TVR) [17]. The secondary variables examined were ACM, MI, and TVR. MI was described as a clinical syndrome with augmented cardiac troponin exceeding the upper reference limit 99th percentile, as well as indication of acute myocardial ischemia [17, 18]. TVR referred to the corresponding TVR via either PCI (stent implantation or angioplasty) or coronary artery bypass grafting (CABG) [17, 18]. Follow-up was conducted via medical record review, outpatient visits, and telephone interviews.

Statistical Analysis

Continuous variables were evaluated with t test for data with a normal distribution and Mann-Whitney U test for the remaining data, and are reported as mean ± standard deviation or median (quartiles), as necessary. Categorical data were evaluated via chi-square or Fisher's exact test, as necessary, and are provided as counts (percentages). Receiver operating characteristic (ROC) curves were generated for post-PCI OFR performance prediction in delineating patients who will and will not develop MACE. The ideal OFR threshold and area under the curve (AUC) were computed. Variables with $P < 0.10$ in univariate Cox analysis were further assessed with multivariate Cox analysis for determination of independent risk factors associated with the primary and secondary endpoints. Survival curves

were evaluated with Kaplan-Meier analysis, and comparison was conducted via the log-rank test. A two-tailed P value <0.05 was deemed significant. All data analyses were performed in SPSS 25.0 (IBM SPSS, Chicago, Illinois), and plots were generated in GraphPad Prism 9.0 (GraphPad Software, Boston, MA).

Results

Baseline Clinical and Vessel Features

As depicted in Figure 2, a total of 457 consecutive patients with CAD who underwent OCT-directed PCI were initially recruited for this study. After selection according to our strict inclusion and exclusion guidelines, 307 patients entered the analyses. The study participants were separated into two cohorts, on the basis of the optimal post-PCI OFR threshold via ROC analysis (Figure 4A), and the baseline profile was classified with the post-PCI OFR threshold, as detailed in Table 1. Patients with OFR ≤0.91 were more susceptible to enhanced multivessel disease rates, as well as a greater stent length, than those with OFR >0.91. The post-PCI OCT results classified by post-PCI OFR threshold are presented in Table 2. Patients with OFR ≤0.91 compared with OFR >0.91 exhibited a greater analyzable OCT image length, enhanced TCFA rate, and smaller average lumen diameter, minimum luminal area (MLA), minimum stent area (MSA), average stent area, minimal stent expansion, and average stent expansion. Table 3 shows the angiography profile classified via post-PCI OFR threshold. Patients with OFR ≤0.91 compared with OFR >0.91 presented greater lesion length and smaller minimum lumen diameter (MLD) of the lesion.

Outcomes

During the median 512 (interquartile range [IQR]: 430–821)-day follow-up, 31 (10.1%) patients exhibited MACE, four expired, 15 had MI, and 12 developed TVR. Among the 15 cases of MI, 12 were confirmed to be target lesion-associated MI, as substantiated by evidence from electrocardiograms, computerized tomography, and coronary angiography. The remaining three cases lacked additional evidence to definitively establish a connection to the target lesion. Of the 12 cases of TVR, nine were identified as ischemia-driven TVR, as supported by coronary functional assessments or intracoronary imaging evidence indicating myocardial ischemia. The other

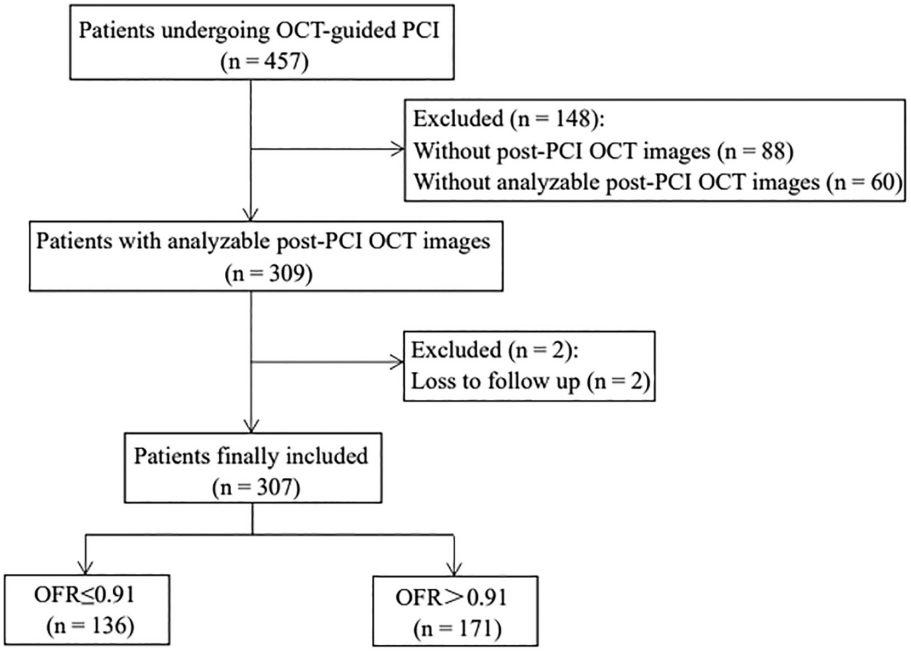

Figure 2 Outline of this Investigation.
OCT: optical coherence tomography; OFR: optical flow ratio; PCI: percutaneous coronary intervention.

Table 1 CAD Patient Baseline Profile, Classified according to post-PCI OFR Threshold Value.

	Overall (n = 307)	OFR ≤0.91 (n = 136)	OFR >0.91 (n = 171)	P value
Male	254 (82.7)	115 (81.3)	139 (84.6)	0.451
Age, years	63 (56–71)	63 (56–72)	63 (55–71)	0.621
BMI, kg/m^2	23.9 (21.8–26.0)	24.2 (22.1–26.3)	23.6 (21.6–25.6)	0.204
Smoking	99 (32.2)	44 (32.4)	55 (32.2)	0.972
Hypertension	190 (61.2)	92 (67.6)	98 (57.3)	0.064
Diabetes mellitus	86 (28.0)	42 (30.9)	44 (25.7)	0.318
Atrial fibrillation	14 (4.6)	5 (3.7)	9 (5.3)	0.508
Prior MI	27 (8.8)	11 (8.1)	16 (9.4)	0.697
Prior PCI	77 (25.1)	37 (27.2)	40 (23.4)	0.444
Prior CABG	1 (0.3)	1 (0.4)	0 (0)	0.908
ACS	66 (21.4)	29 (21.3)	37 (21.6)	0.947
Antiplatelet therapy	306 (99.7)	135 (99.3)	171 (100)	0.908
Oral anticoagulation	9 (2.9)	4 (2.9)	5 (2.9)	1.000
Laboratory data				
LDL-C, mg/dL	2.6 (2.1–3.3)	2.7 (2.1–3.3)	2.6 (2.0–3.3)	0.926
Creatinine, mg/dL	81.7 (70.4–96.0)	83.5 (71.2–98.3)	80.7 (68.0–95.9)	0.120
HGB, g/L	134 (121–144)	133 (120–142)	135 (121–147)	0.108
CK-MB, U/L	12.0 (10.0–15.8)	12.0 (10.0–15.7)	11.9 (10.0–16.0)	0.671
LVEF, %	63 (58–67)	62 (58–67)	63 (58–67)	0.441
Radial approach	287 (93.5)	125 (91.9)	162 (94.7)	0.319
Lesion location				0.673
LAD	178 (58.0)	80 (58.8)	98 (57.3)	
LCX	30 (9.8)	11 (10.5)	19 (3.2)	
RCA	99 (32.2)	45 (32.6)	54 (29.0)	
Multivessel disease	190 (61.9)	93 (68.4)	97 (56.7)	0.037
Multiple stents	105 (34.2)	52 (38.2)	53 (31.0)	0.184
Stent length, mm	31 (22–40)	33 (26–41)	29 (21–40)	0.014

Data are median (IQR) or n (%). ACS: acute coronary syndrome; BMI: body mass index; CABG: coronary artery bypass grafting; CAD: coronary artery disease; CK-MB: creatine kinase-MB isoenzyme; HGB: hemoglobin; LAD: left anterior descending artery; LCX: left circumflex artery; LDL-C: low density lipoprotein cholesterol; LVEF: left ventricular ejection fraction; MI: myocardial infarction; OFR: optical flow ratio; PCI: percutaneous coronary intervention; RCA: right coronary artery.

three cases were classified as angiography-driven TVR, solely on the basis of on findings from coronary angiography. An OFR ≤0.91 was strongly associated with enhanced MACE (18.38% vs 3.51%, P < 0.0001), MI (9.56% vs 1.17%, P < 0.001), and TVR (6.62% vs 1.75%, P < 0.05) incidence (Figure 3).

MACE Predictive Performance of Post-PCI OFR

On the basis of our post-PCI OFR ROC curve that predicted future MACE in patients, the optimal OFR threshold was 0.91, and the AUC was 0.702 (95% confidence interval [CI]: 0.608–0.795; P < 0.001; sensitivity: 80.6%; specificity: 59.8%) (Figure 4A). The incremental post-PCI OFR values for MACE recognition according to the baseline profiles and OCT results were also validated. In relation to model 1 (baseline characteristics plus OCT results), model 2 (model 1 plus post-PCI OFR) displayed greater MACE discrimination (AUC: 0.772, 95% CI: 0.721–0.818 vs AUC: 0.675, 95% CI: 0.620–0.727; P = 0.007) (Figure 4B).

MACE-Related Factors

Table 4 summarizes the uni- and multivariate analyses results for MACE among patients with CAD

Table 2 Post-PCI OCT Results in Patients with CAD, Classified according to post-PCI OFR Threshold Value.

	Overall (n = 307)	OFR ≤ 0.91 (n = 136)	OFR > 0.91 (n = 171)	P value
Target vessel				
Length of analyzable images, mm	52.4 (45.5–56.8)	53.9 (48.2–64.6)	50.8 (43.5–53.9)	<0.001
Mean lumen diameter, mm	3.1 (2.8–3.5)	2.8 (2.6–3.0)	3.4 (3.1–3.7)	<0.001
MLA, mm^2	5.6 (4.3–7.0)	4.4 (3.6–5.3)	6.6 (5.4–8.0)	<0.001
Stented segment				
MSA, mm^2	5.4 (4.4–6.6)	4.6 (3.7–5.4)	6.4 (5.1–7.9)	<0.001
Mean stent area, mm^2	8.3 (6.8–9.9)	6.8 (5.9–8.1)	9.5 (8.2–11.1)	<0.001
Minimal stent expansion, %	59.0 (50.0–68.0)	52.5 (48.0–63.0)	64.0 (56.0–73.0)	<0.001
Mean stent expansion, %	87.0 (77.0–100.0)	81.0 (71.0–91.8)	93.0 (83.0–105.0)	<0.001
Irregular protrusion	162 (52.8)	72 (52.9)	90 (52.6)	0.957
Stent malapposition	182 (59.3)	73 (53.7)	109 (63.7)	0.075
Reference segments + nonculprit lesion				
Qualitative findings				
TCFA	180 (58.6)	90 (66.2)	90 (52.6)	0.017
Stent edge dissection	52 (16.9)	27 (19.9)	25 (14.6)	0.225

Data are median (IQR) or n (%). MLA: minimum lumen area; MSA: minimum stent area; OCT: optical coherence tomography; TCFA: thin-cap fibroatheroma; other abbreviations as in Table 1.

Table 3 Angiography Profiles of Patients with CAD, Classified according to post-PCI OFR Threshold Value.

	Overall (n = 307)	OFR ≤0.91 (n = 136)	OFR >0.91 (n = 171)	P value
Lesion length, mm	27.2 (15.6–44.2)	35.4 (20.0–49.8)	23 (12.0–36.4)	<0.001
Lesion MLD, mm	1.54 (1.21–2.03)	1.44 (1.12–1.92)	1.71(1.28–2.15)	0.044
Reference vessel diameter, mm	2.66(1.91–4.81)	2.48(1.81–3.79)	2.95(2.11–5.27)	0.100
DS, %	57.1(44.8–63.4)	58.0(45.6–63.7)	56.7(44.5–63.3)	0.501

DS: diameter stenosis; MLD: minimum lumen diameter; other abbreviations as in Table 1.

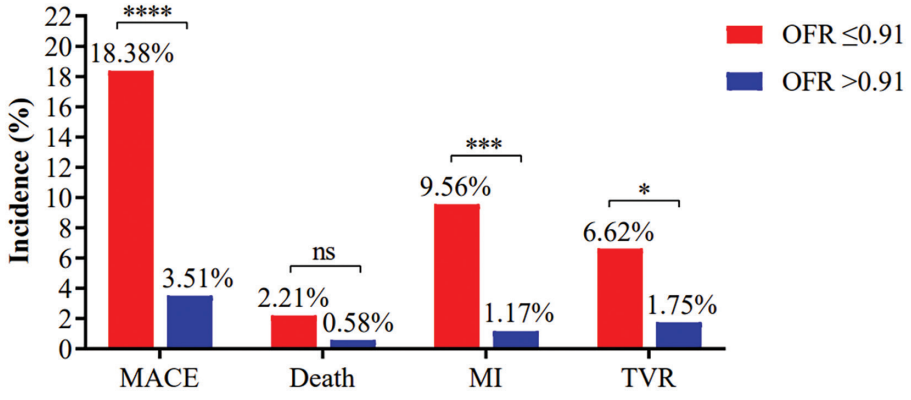

Figure 3 Distinct post-PCI OFR Patient Prognoses.
****P < 0.0001, ***P < 0.001, *P < 0.05, ns: not significant. MACE: major adverse cardiovascular events; TVR: target vessel revascularization; other abbreviations as in Table 1.

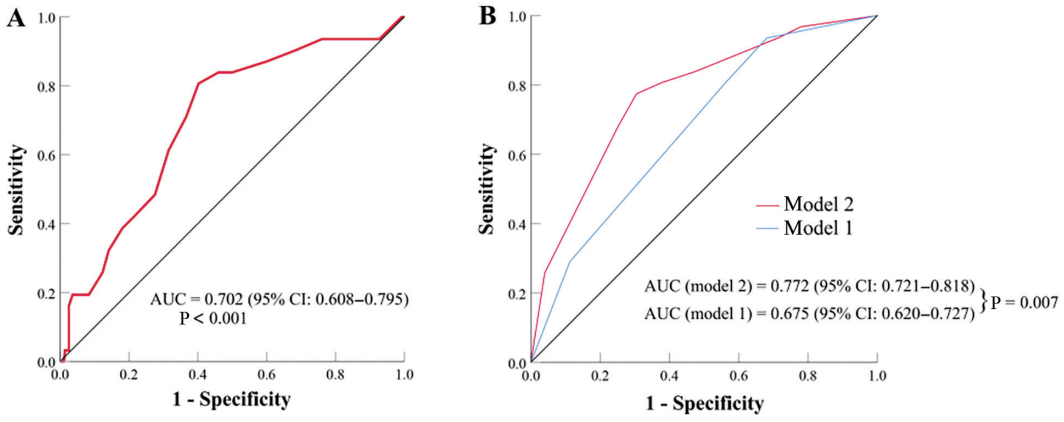

Figure 4 The ROC Curves of (A) Post-PCI OFR for Identification of Patients with CAD with MACE, and (B) Predictive Models for MACE.
Model 1 denotes baseline profiles and OCT results, and model 2 denotes model 1 and post-PCI OFR. AUC: area under the curve; CI: confidence interval; MACE: major adverse cardiovascular events; ROC: receiver operating characteristic; other abbreviations as in Table 1 and Table 2.

Table 4 MACE Cox Regression Analyses of Patients with CAD after PCI.

	Univariate analysis			Multivariate analysis		
	HR	95% CI	P value	HR	95% CI	P value
Prior PCI	2.29	1.12–4.68	0.023	2.75	1.31–5.78	0.008
OFR ≤0.91	6.31	2.58–15.43	<0.001	3.60	1.24–10.44	0.019
Mean lumen diameter ≤3.17 mm	4.03	1.65–9.86	0.002	1.59	0.50–5.02	0.428
MLA ≤4.40 mm^2	4.47	2.18–9.15	<0.001	2.17	0.85–5.56	0.106
MSA ≤5.06 mm^2	3.26	1.53–6.95	0.002	1.19	0.44–3.22	0.735
TCFA	3.20	1.31–7.81	0.011	3.63	1.42–9.20	0.007

CI: confidence interval; HR: hazard ratio; MACE: major adverse cardiovascular events; other abbreviations as in Table 1 and Table 2.

after PCI. On the basis of our multivariate analysis, an OFR ≤0.91 (hazard ratio [HR]: 3.60; 95% CI: 1.24–10.44; P = 0.019), as well as prior PCI (HR: 2.75; 95% CI: 1.31–5.78; P = 0.008) and TCFA (HR: 3.63; 95% CI: 1.42–9.20; P = 0.007), were strong independent MACE indicators. Using survival curves, we further demonstrated that the MACE incidence was substantially elevated among individuals with OFR ≤0.91, relative to those with elevated OFR >0.91 (log-rank P < 0.001) (Figure 5A). Moreover, individuals with TCFA had a greater MACE incidence than those without TCFA (log-rank P = 0.007) (Figure 5B).

Factors Associated with ACM, MI, and TVR

Our multivariate analysis for the secondary outcomes revealed that OFR ≤0.91 was a robust independent risk factor for MI (HR: 14.64; 95% CI: 3.27–65.54; P < 0.001) (Table 5). However, we observed no association between OFR and ACM or TVR (Tables 6 and 7). Using survival analysis, we demonstrated that the MI incidence was considerably greater among patients with OFR ≤0.91 than OFR >0.91 (log-rank P < 0.001) (Figure 6).

Discussion

The conclusion of our investigation are as follows. (1) The optimal post-PCI OFR threshold of MACE was 0.91, and combining OFR with OCT results augmented the predictive performance of MACE after PCI. (2) Patients with OFR ≤0.91 and TCFA exhibited enhanced MACE incidence, and the MI incidence was also substantially greater among patients with OFR ≤0.91 than OFR >0.91. Finally, (3) OFR ≤0.91 and TCFA were independent

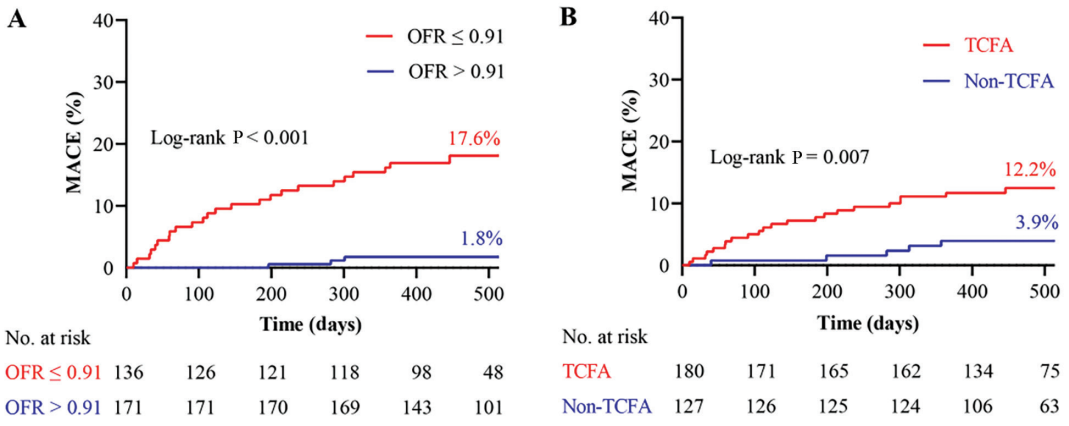

Figure 5 Kaplan-Meier Survival Curves of MACE Among Patients with CAD, on the Basis of (A) Post-PCI OFR and (B) TCFA.
MACE: major adverse cardiovascular events; other abbreviations as in Table 1 and Table 2.

Table 5 MI Cox Regression Analyses of Patients with CAD after PCI.

	Univariate analysis			Multivariate analysis		
	HR	95% CI	P value	HR	95% CI	P value
OFR ≤0.91	11.85	2.67–52.55	0.001	14.64	3.27–65.54	<0.001
Malapposition	3.10	0.87–11.01	0.081	4.51	1.25–16.29	0.022
MLA, mm^2	0.72	0.55–0.95	0.019			
MSA, mm^2	0.60	0.42–0.86	0.005			
TCFA	3.14	0.89–11.15	0.076			

CI: confidence interval; HR: hazard ratio; other abbreviations as in Table 1 and Table 2.

Table 6 ACM Cox Regression Analyses of Patients with CAD after PCI.

	Univariate analysis			Multivariate analysis		
	HR	95% CI	P value	HR	95% CI	P value
Age, years	1.13	1.01–1.26	0.031			
ACS	10.46	1.09–100.81	0.042	11.39	1.02–127.30	0.048
HGB, g/L	0.94	0.90–0.98	0.009	0.92	0.50–5.02	0.008
Length of analyzable images, mm	1.10	1.00–1.21	0.051			
Minimal stent expansion, %	1.05	1.01–1.09	0.007	1.05	1.01–1.11	0.031

ACM: all-cause mortality; CI: confidence interval; HR: hazard ratio; other abbreviations as in Table 1.

indicators of MACE, and OFR ≤0.91 was also an independent indicator of MI.

Prognostic Performance of Post-PCI OFR among Patients with CAD

Owing to substantial inconsistency between angiographic and functional severity [19, 20], FFR is typically indicated to increase the physiological importance of coronary artery stenosis [1]. Pressure wire-based FFR measurement is well established to require complete microvascular vasodilation for maximal hyperemia induction [21]. Microcirculatory dysfunction during MI may negative influence maximal hyperemia, thereby skewing FFR measurement precision [5, 22]. Alternatively, OFR facilitates relatively rapid OCT image-based FFR calculation without requiring pressure wires

Table 7 TVR Cox Regression Analyses of Patients with CAD after PCI.

	Univariate analysis			Multivariate analysis		
	HR	95% CI	P value	HR	95% CI	P value
LDL-C, mg/dL	0.42	1.01–1.26	0.031	0.42	0.19-0.91	0.028
OFR ≤0.91	4.18	1.13–15.47	0.032			
MLA, mm^2	0.54	0.36–0.82	0.004			
Mean lumen diameter, mm	0.83	0.19–0.36	0.001	0.13	0.03-0.51	0.003
MSA, mm^2	0.63	0.41–0.95	0.027			
Mean stent area, mm^2	0.74	0.55–0.99	0.047			
TCFA	3.70	0.81–16.89	0.091			

CI: confidence interval; HR: hazard ratio; TVR: target vessel revascularization; other abbreviations as in Table 1 and Table 2.

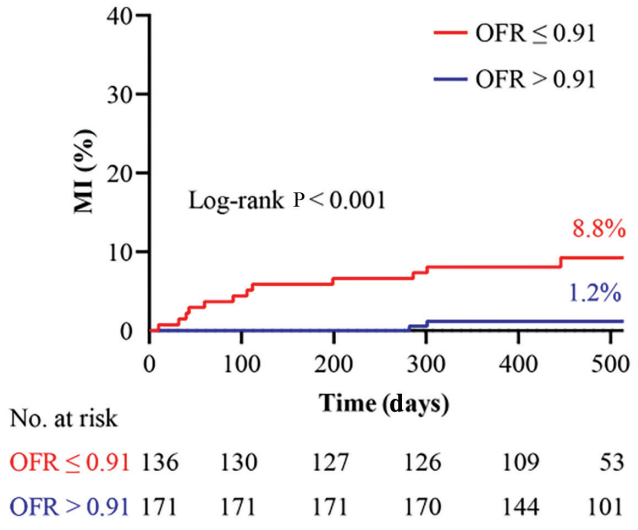

Figure 6 Kaplan-Meier Survival Curves of MI among Patients with CAD, on the Basis of post-PCI OFR. Abbreviations as in Table 1.

and induced hyperemia [15]. Therefore, in patients in acute condition, namely, those with ACS, OFR measurement is a better choice than FFR measurement. More importantly, prior investigations have reported acceptable diagnostic concordance of OFR with FFR [6, 23] and in fact have revealed a close link between diminished FFR after PCI and poorer cardiovascular prognosis in patients with ACS or CAD, even with differing FFR thresholds [5, 17, 18]. Herein, we reported an optimal post-PCI OFR threshold for MACE of 0.91, corroborating prior findings [7, 17]. In addition, Shunsuke Kakizaki et al. have revealed that diminished vessel-level OFR alone is intricately associated with target vessel failure, an integrated endpoint of cardiac mortality, TV-associated MI, and ischemic TVR, after PCI among patients with ACS [7]. Likewise, other studies have reported OFR as a robust independent indicator of nonculprit vessel-associated MACE among patients with ACS [12]. Herein, we demonstrated that post-PCI OFR is an independent predictor of MACE as well as MI among patients with CAD. Collectively, these results highlight the potential of OFR after PCI in predicting long-term outcomes of patients with CAD.

Clinical Relevance of Combining OFR and OCT Findings after PCI

Several reports have indicated that aberrant OCT results after stent placement, for example, irregular protrusion, small MSA, in-stent MLA <4.5 mm^2, and distal SED, are strongly correlated with poor clinical outcomes [9, 11]. These findings have confirmed the prognostic relevance of OCT among patients after PCI. In addition, OCT enables the identification of high-risk vulnerable plaque profiles, for example, TCFA [24, 25]. Herein, similarly to earlier investigations, we revealed that TCFA is intricately associated with MACE [25, 26]. However, such morphological assessments are both time-consuming and subjective. Emerging evidence suggests that small MLA and SED at the proximal reference segment are strongly and independently correlated with diminished vessel-level OFR [7]. In this report, we revealed that individuals with low post-PCI OFR generally exhibited poorer OCT results, and combining OFR with OCT results enhanced MACE prediction. Therefore, OFR measurement after PCI is highly beneficial for the detection of unfavorable OCT morphological profiles, which in turn can

identify patients with poor prognosis. We recommend an extensive morphological and functional evaluation of coronary stenosis by using OCT imaging for detecting vessels in need of additional revascularization. Enhancement of this technique may potentially optimize PCI and improve consequences associated with cardiovascular events.

Study Limitations

This study has several limitations. First, this retrospective investigation involved a relatively small Chinese patient population from an individual center. Thus, additional prospective investigations involving multiple centers and larger sample population are warranted to confirm our findings. Second, we analyzed ACM and not cardiovascular mortality, thus potentially limiting the detailed analyses of mortality causes. Third, the OCT image morphological evaluation was subjective; this aspect is an intrinsic limitation of OCT imaging. Fourth, the discrepancy in the length of analyzable images between the OFR >0.91 and <0.91 groups might have affected the analyzable number of side branches and potentially contributed to a different pressure drop. Finally, we examined only the population of patients with CAD. In future, exploration of the prognosis of different categories of patients with CAD, as well as culprit and nonculprit vessels, will be imperative.

Conclusion

Post-PCI OFR was found to be an independent MACE indicator among patients with CAD. Combining OFR and OCT results may enhance MACE detection after PCI. Therefore, integrating OCT morphology with physiology is a promising approach to improving cardiovascular outcomes among patients with CAD.

Data Availability Statement

The research data are available from the corresponding author upon reasonable request. The data are not publicly available, to protect patient privacy.

Ethics Statement

The study was conducted in accordance with the Declaration of Helsinki and was approved by the Scientific Research Ethics Committee of Guangdong Provincial People's Hospital (KY-Q-2022-091-01).

Author Contributions

Conceptualization, C.H.; methodology, C.H. and S.C.; software, C.H., S.C., T.H., and ZH.L.; validation, S.C., T.H., P.C., and ZJ.L.; formal analysis, C.H., S.C., T.H., and ZH.L.; investigation, C.H. and S.C.; resources, C.H., S.C., and T.H.; data curation, C.H., S.C., and P.C.; writing – original draft preparation, C.H. and S.C.; writing – review and editing, T.H., ZH.L., P.C., ZJ.L., L.X., Y.L., and P.H.; visualization, C.H. and S.C.; supervision, Y.L. and P.H.; project administration, Y.L. and P.H.; funding acquisition, P.H.

Funding

This work was supported by the Outstanding Young Talent Program of Guangdong Provincial People's Hospital (grant number KJ012019084) and the High-level Hospital Construction Project (grant number DFJH2020021).

Conflict of Interest

The authors declare no conflicts of interest.

REFERENCES

1. Neumann FJ, Sousa-Uva M, Ahlsson A, Alfonso F, Banning AP, Benedetto U, et al. 2018 ESC/EACTS Guidelines on myocardial revascularization. Eur Heart J 2019;40(2):87–165.
2. Räber L, Mintz GS, Koskinas KC, Johnson TW, Holm NR, Onuma Y, et al. Clinical use of intracoronary imaging. Part 1: guidance and optimization of coronary interventions. An expert consensus document of the European Association of Percutaneous Cardiovascular Interventions. Eur Heart J 2018;39(35):3281–300.
3. Takahashi T, Shin D, Kuno T, Lee JM, Latib A, Fearon WF, et al.

Diagnostic performance of fractional flow reserve derived from coronary angiography, intravascular ultrasound, and optical coherence tomography; a meta-analysis. J Cardiol 2022;80(1):1–8.
4. Hu MJ, Tan JS, Yin L, Zhao YY, Gao XJ, Yang JG, et al. Clinical outcomes following hemodynamic parameter or intravascular imaging-guided percutaneous coronary intervention in the era of drug-eluting stents: an updated systematic review and Bayesian network meta-analysis of 28 randomized trials and 11,860 patients. Front Cardiovasc Med 2022;9:860189.
5. Tu S, Westra J, Adjedj J, Ding D, Liang F, Xu B, et al. Fractional flow reserve in clinical practice: from wire-based invasive measurement to image-based computation. Eur Heart J 2020;41(34):3271–9.
6. Hu F, Ding D, Westra J, Li Y, Yu W, Wang Z, et al. Diagnostic accuracy of optical flow ratio: an individual patient-data meta-analysis. EuroIntervention 2023;19(2):e145–54.
7. Kakizaki S, Otake H, Seike F, Kawamori H, Toba T, Nakano S, et al. Optical coherence tomography fractional flow reserve and cardiovascular outcomes in patients with acute coronary syndrome. JACC Cardiovasc Interv 2022;15(20):2035–48.
8. Zhang M, Matsumura M, Usui E, Noguchi M, Fujimura T, Fall KN, et al. Intravascular ultrasound-derived calcium score to predict stent expansion in severely calcified lesions. Circ Cardiovasc Interv 2021;14(10):e010296.
9. Soeda T, Uemura S, Park SJ, Jang Y, Lee S, Cho JM, et al. Incidence and clinical significance of poststent optical coherence tomography findings: one-year follow-up study from a multicenter registry. Circulation 2015;132(11):1020–9.
10. Bryniarski KL, Tahk SJ, Choi SY, Soeda T, Higuma T, Yamamoto E, et al. Clinical, angiographic, IVUS, and OCT predictors for irregular protrusion after coronary stenting. EuroIntervention 2017;12(18):e2204–211.
11. Prati F, Romagnoli E, La Manna A, Burzotta F, Gatto L, Marco V, et al. Long-term consequences of optical coherence tomography findings during percutaneous coronary intervention: the Centro Per La Lotta Contro L'infarto - Optimization Of Percutaneous Coronary Intervention (CLI-OPCI) LATE study. EuroIntervention 2018;14(4):e443–51.
12. Hong H, Jia H, Zeng M, Gutiérrez-Chico JL, Wang Y, Zeng X, et al. Risk stratification in acute coronary syndrome by comprehensive morphofunctional assessment with optical coherence tomography. JACC Asia 2022;2(4):460–72.
13. Karanasos A, Tu S, van Ditzhuijzen NS, Ligthart JM, Witberg K, Van Mieghem N, et al. A novel method to assess coronary artery bifurcations by OCT: cut-plane analysis for side-branch ostial assessment from a main-vessel pullback. Eur Heart J Cardiovasc Imaging 2015;16(2):177–89.
14. Tu S, Echavarria-Pinto M, von Birgelen C, Holm NR, Pyxaras SA, Kumsars I, et al. Fractional flow reserve and coronary bifurcation anatomy: a novel quantitative model to assess and report the stenosis severity of bifurcation lesions. JACC Cardiovasc Interv 2015;8(4):564–74.
15. Yu W, Huang J, Jia D, Chen S, Raffel OC, Ding D, et al. Diagnostic accuracy of intracoronary optical coherence tomography-derived fractional flow reserve for assessment of coronary stenosis severity. EuroIntervention 2019;15(2):189–97.
16. Chu M, Jia H, Gutiérrez-Chico JL, Maehara A, Ali ZA, Zeng X, et al. Artificial intelligence and optical coherence tomography for the automatic characterisation of human atherosclerotic plaques. EuroIntervention 2021;17(1):41–50.
17. Kasula S, Agarwal SK, Hacioglu Y, Pothineni NK, Bhatti S, Ahmed Z, et al. Clinical and prognostic value of poststenting fractional flow reserve in acute coronary syndromes. Heart 2016;102(24):1988–94.
18. Agarwal SK, Kasula S, Hacioglu Y, Ahmed Z, Uretsky BF, Hakeem A. Utilizing post-intervention fractional flow reserve to optimize acute results and the relationship to long-term outcomes. JACC Cardiovasc Interv 2016;9(10):1022–31.
19. Tonino PA, Fearon WF, De Bruyne B, Oldroyd KG, Leesar MA, Ver Lee PN, et al. Angiographic versus functional severity of coronary artery stenoses in the FAME study fractional flow reserve versus angiography in multivessel evaluation. J Am Coll Cardiol 2010;55(25):2816–21.
20. Park SJ, Kang SJ, Ahn JM, Shim EB, Kim YT, Yun SC, et al. Visual-functional mismatch between coronary angiography and fractional flow reserve. JACC Cardiovasc Interv 2012;5(10):1029–36.
21. Toth GG, Johnson NP, Jeremias A, Pellicano M, Vranckx P, Fearon WF, et al. Standardization of fractional flow reserve measurements. J Am Coll Cardiol 2016;68(7):742–53.
22. Cuculi F, De Maria GL, Meier P, Dall'Armellina E, de Caterina AR, Channon KM, et al. Impact of microvascular obstruction on the assessment of coronary flow reserve, index of microcirculatory resistance, and fractional flow reserve after ST-segment elevation myocardial infarction. J Am Coll Cardiol 2014;64(18):1894–904.
23. Seike F, Uetani T, Nishimura K, Kawakami H, Higashi H, Aono J, et al. Intracoronary optical coherence tomography-derived virtual fractional flow reserve for the assessment of coronary artery disease. Am J Cardiol 2017;120(10):1772–9.
24. Kubo T, Ino Y, Mintz GS, Shiono Y, Shimamura K, Takahata M, et al. Optical coherence tomography detection of vulnerable plaques at high risk of developing acute coronary syndrome. Eur Heart J Cardiovasc Imaging 2021.
25. Prati F, Romagnoli E, Gatto L, La Manna A, Burzotta F, Ozaki Y, et al. Relationship between coronary

plaque morphology of the left anterior descending artery and 12 months clinical outcome: the CLIMA study. Eur Heart J 2020;41(3):383–91.

26. Kedhi E, Berta B, Roleder T, Hermanides RS, Fabris E, IJsselmuiden AJJ, et al. Thin-cap fibroatheroma predicts clinical events in diabetic patients with normal fractional flow reserve: the COMBINE OCT-FFR trial. Eur Heart J 2021;42(45):4671–9.